EFFECTS OF SOFT SOIL ON BUILDING RESPONSE IN MEXICO CITY

G. Waas[1]

ABSTRACT

Ground motions recorded in Mexico City on Sept. 19, 1985 are compared with results from soil amplification analyses using one- dimensional theory. Resonant effects between soil layers and a typical 10-floor office building are illustrated by analysis. The influence of pile foundations on the response of buildings is addressed. An analysis method for pile groups subjected to earthquake motion is outlined, which handles layered soil and pile-soil-pile interaction.

INTRODUCTION

The recent earthquake of Loma Prieta in California at Oct. 17, 1989 has demonstrated again that earthquake damage tends to be larger on soft soil than on stiff ground. There are several reasons for this: Subsidence of loose granular soils or liquefaction of water-satured sands and silts may add to the distress of the shaken structures. Soft soil layers over stiffer strata amplify the ground motion in certain frequency ranges. This latter affect has never been more pronounced than in the great quake of September 19, 1985 in Mexico City, where it led to the collaps of hundreds of tall buildings located on the tick clay layers in the center of the city, whereas no damage was observed in the areas with hard ground.

This paper presents results from one-dimensional wave propagation theory applied to typical soil profiles in the center of Mexico City. It illustrates the observed resonance of highrise building with the fundamental natural frequency of the clay layers and it addresses soil-structure interaction of pile foundations and its effect on building response.

SOIL AMPLIFICATION

In the earthquake of Sept. 19, 1985 ground accelerations in Mexico City reached only 0,3 to 0,4 m/s^2 on hard ground as recorded at Ciudad Universitaria (CU) and Tacubaya (Tac), whereas on the soft clay deposits in the center of the city peak ground accelerations between 1 and 2 m/s^2 were measured.

The amplification of horizontal ground motion may be explained qualitatively and also quantitatively and also quantitatively by simple one-dimensional wave theory. Vertically

[1] Hochtief AG, Abt IKS, Bockenheimer Landstr 24 D-6000 Frankfurt/main, Germany

propagating shear waves are considered which are generated by predominantly long period motion of the rock strata underlying the gravel, sand and clay layers. The two different profiles shown in Fig. 1 are used; they were originally developed by Rosenblueth [2] in 1969 for a similar study. The two top layers represent very soft and soft clay layers followed by sand and gravel and partially cemented valley sediments.

As input motion at the bottom of the profiles, the acceleration time histories recorded at CU and Tac are applied as waves impinging vertically from below. The amplitudes of the incident waves are taken as half of those recorded at CU and Tac. Thus the doubling of amplitudes of vertically propagating waves by reflection at the free ground surface (at CU and Tac) is taken into account.

Figure 2 shows the acceleration response spectra at 5% damping for the motion at CU an Tac and for the motion at the top of the two soil profiles as computed using the CU and Tac accelerations as input at the base of the profiles. Also shown in Fig. 2 is the spectrum for the acceleration recorded at ground surface near the Secretaria de Comunicaciones y Transportes (SCT) on a soil profile typical for the center of the city.

The comparison of the spectra for hard ground and soft soil shows an amplification of 5 to 6 at low periods and of roughly 10 to 20 at the period of 2 seconds. Near this period the soil profiles show a pronounced resonant period. The spectra of the motion computed by the one-dimensional wave propagation theory agree quite well with the spectrum of the acceleration recorded at the SCT. The fundamental period at around two seconds and the height of the response peak is well matched by the simple theory using profiles with data that appear consistent with actual soil profiles and measured soil properties.

Based on similar analyses using different values for the thickness and shear wave velocity of the sand and gravel deposits, it is tentatively concluded that the deposits underlying the clay layers may have a significant effect on the amount of amplification at periods around 2 seconds. The very large motion in the center of Mexico City may possibly result from resonant effects due to similar natural periods of the clay layers and the underlying sediment.

RESONANCE OF BUILDINGS AND GROUND VIBRATIONS

The fact that tall buildings with approximately 7 to 13 floors suffered much more damage and collapses than lower or very high buildings in the center of Mexico City indicates that resonance between the ground motion and the fundamental vibration periods of these buildings (7 to 13 floors) was a mayor cause for destruction.

The following example calculation illustrates the resonant effects. Figure 4 shows the narrow side of a typical office building with 10 floors. It is a concrete frame structure with a plan of 15 m by 50 m supported by 4 x 11 cast-in-place concrete piles of 0,90 m diameter and 30 m length. The piles are assumed to be fixed in a fairly rigid pile cap. The fundamental period of the structure is 1.1 s for the case of a totally fixed foundation. If the flexibility of the pile foundation is considered, the

fundamental period of the structure increases to 1.9 s and is thus very close to the fundamental period of the ground. The soil profile is almost the same as that of profile 1 in Fig. 1.

The flexibility of the pile foundation and its contribution to the fundamental period of the building is mainly due to bending of the vertical piles when subjected to a horizontal base shear force of the structure. The rocking stiffness of the pile foundation, even in the shorter direction, is relatively large and therefore has only a small influence on the fundamental period of the building.

The pile foundation and the structure are excited by vertically propagating shear waves in the profile. These waves are generated at the base of the profile (-500m) by horizontal acceleration, which are consistens with vertically incident shear waves from below.

Figure 4 shows how the accelerations increase from the basè profile to the roof of the building. There is already a marked increase of the motion from -500m to the top of the sand and gravel deposits at -26m, it is roughly a factor of 2.6. From there to the free ground surface the motion increases further by a factor of approximately 2.7. The stiffness of the piles reduce the motion slightly if there is no building mass. Finally, the motion increases with the height of the building; the factor between the pile cap and the roof is three.

In this analysis the structure was considered to respond linearly to the excitation, having 5% of viscous damping. At this level of shaking the response of the structure would be in reality inelastic. Thus the amplification of motion from the pile cap to the roof would be less than show in Fig. 4.

The difference of the free field ground surface motion and the motion of the pile cap without the building depends generally on the bending stiffness of the pile, the pile spacing and the number of piles. In this case, as in most cases, the difference is small, see Fig. 5.

In the present examples the dynamic analysis of the soil strata, the pile foundations, and the structure is performed via the frequency domain. Transfer functions are computed using the complex response method, and time histories are computed by Fast Fourier Transform Techniques (FFT).

The interaction of the pile foundation with the soil is analyzed by a quite sophisticated method, which is from the engineering mechanics point of view rather rigorous as long as the soil and the piles stay in the linear response range. It considers the three-dimensional situation and takes pile-soil-pile interaction into account. It is briefly outlined below.

METHOD OF ANALYSIS FOR PILE GROUPS

Displacements, shear forces and bending moments shall be computed for a group of piles which are subjected to horizontal and vertical loads. The loads may be static or dynamic forces, prescribed displacements or accelerations. Pile-soil-pile interaction is taken into account.

The soil is horizontally layered; it extends laterally to infinity and is underlain by a rigid base or an approximation of an elastic halfspace by viscous dampers at a finite depth. The soil is treated as a linear elastic or visco-elastic medium using complex modules representation. Non-linear soil behavior may be approximated by adjusting iteratively the module and damping values to computed strain levels in each soil layer.

The piles consist of vertical beam elements with linear bending and shear behavior including material damping. The location of the piles in plan is arbitrary. Symmetry properties may be utilized to reduce the required storage and computational effort. The piles are pinned or fixed at the pile cap which may be assumed rigid for simplicity in many cases.

Procedure.

Each pile is connected to the soil at several, say 10 to 20, nodes as indicated in Figs. 1 and 2 of the Appendix. Displacements and rotations of the soil and the piles are matched at these nodes and equilibrium is enforced. To this end, the soil and the piles are considered as substructures. First, the displacement field caused by time harmonic ring loads in a layered visco-elastic medium is computed as outlined in the appendix. Fig. 3 of the Appendix shows the displacements due to a ring load p. cos in the radial direction. Corresponding figures for a tangential load p.sin and a vertical load p.cos would look similar.

Second, the soil displacement caused by unit loads acting at each node, one at a time, are evaluated for all the nodes where the piles and the soil are to be connected. This leads to the frequency dependent flexibility matrix of the soil, [F].

When flexibility terms are computed that relate forces and displacements at one and the same pile, ring loads with a resultant force or moment of unit value in the respective direction are applied along the periphery of the pile at a nodal ring (node). Displacements and rotations are computed similarly along the periphery of the pile. For the resultant nodal displacements it is assumed that the circular cross section of a pile does not deform. When flexibility terms are computed that relate displacements and forces at different piles, the ring loads are reduced to point loads and the displacements are computed for the axis of a pile rather than for its periphery. Furthermore, vertical displacements of the soil around one pile caused by forces acting at another pile are disregarded for simplicity.
Next, the flexibility matrix of the piles, [F], is computed. Since the flexibility matrix of the soil does not take the boreholes in the soil into account, one may deduct the mass and stiffness of the soil within the pile cross-section from those of the actual pile.
Finally, the soil and the piles are connected at the common nodes. This leads to

$$([F_s] + [F_p])\ \{P_i\} = [F_p]\ \{P_e\} \qquad (1)$$

$$[F_p]\ (\{P_e\} - \{P_i\}) = \{u\} \qquad (2)$$

$$[F_s]\ \{P_i\} = \{u\} \qquad (3)$$

Where $\{P_e\}$ = external loads, $\{P_i\}$ = internal forces between soil and piles, and $\{u\}$ = displacements of pile nodes. The matrices and vectors are complex valued, representing amplitudes and phases of harmonic motion at given frequency. $[F_s]$ includes radiation and material damping as well as inertia forces of the soil. [Fp] may include damping and inertia forces of the piles and pile cap mass.

Instead of using the flexibility formulation one can invert the soil flexibility matrix and use a more convenient stiffness formulation for further analysis.

However, $[F_s]$ may be a large matrix which is not sparse, even though the influence of nodal rotations on other piles is neglected and the interaction effects of distant piles may be omitted in some cases. $[F_s]$ for 20 piles with each 10 nodes has more than 400 times 400 complex elements. Therefore an inversion would require a significant effort that can be avoided by the flexibility formulation.

Handling of Symmetry

For simple and double symmetric pile arrangements the dimension of {P} and {u} in Eqs. 1 to 3 can be reduced to half or a quarter respectively. In case of an axisymmetric pile arrangement, the dimension of {P} and {u} may be reduced by a Fourier expansion in the tangential direction. If a rigid pile cap is subjected to a horizontal force or excitation by vertical propagating shear waves of an earthquake, the dimension of {P} and {u} can be reduced to two translational and two rotational degrees of freedom per pile ring and nodal depth. This is equivalent to the degrees of freedom of one pile per pile ring. Along each pile ring, forces and displacements vary elliptically at constant depth. This holds strictly only of the spacing of piles within one ring is constant and if each ring has the same number of piles. In practical cases of circular pile foundations the assumption of an elliptic variation in the tangential direction is a fair approximation, which reduces the numerical effort markedly.

Earthquake Excitation

Earthquake excitation is included in the form of vertically propagating shear waves. They are generated in the model by horizontal acceleration of the bottom boundary. First, the free field motion, $\{u_p\}$ of the soil layers (without the pile foundation) is computed. This is a simple one-dimensional analysis. Then $\{u_f\}$ has to be subtracted on the righthand sides of Eqs. 1 and 3. In case of no external forces $\{P_e\}$ this yields:

$$([F_s] + [F_p])\ \{P_i\} = -\ \{u_F\} \tag{4}$$

$$-\ [F_p]\ \{P_i\} = \{u\} \tag{5}$$

$$[F_s]\ \{P_i\} = \{u\} - \{u_F\} \tag{6}$$

Where {u} is the total displacement.

INTERACTION OF SOIL AND PILES GROUPS

The analysis method outlined above is used to compute the static and dynamic stiffness of a single pile and group of 44 piles (4 x 11) with a spacing of 5 m. The piles are of concrete (25 Mpa), they have a length of 30 m and are fixed at the pile head.

The diameter of the piles is varied. Table 1 summarizes the values of the stiffness for horizontal displacement and rotation of the rigid pile cap about the longer horizontal axis. The rocking stiffness is large and hardly affects the fundamental mode of a 10-floor building. The horizontal stiffness of the single pile and the pile group increases only at a moderate rate with increasing pile diameter. The static group factor is the stiffness ratio of a group and a single pile divided by the number of piles in the group. It is below 0.4 in all cases.

Figure 6 shows the variation of the dynamic stiffness with frequency for a single and a pile group. The stiffness of a single pile is almost constant in the frequency range shown. However, the stiffness of the pile group changes; with increasing frequency, it first drops to about 50% of its static value at the resonant frequency of the soil profile and then grows to values which are larger than the stiffness of a single pile multiplied by the number of piles. The dynamic group factor is larger than one. This is due to pile-soil-pile interaction. While at low frequencies the interaction of piles in group reduces their stiffness, it increases their stiffness at higher frequencies.

Transfer functions for the horizontal motion of the pile foundation without building mass, as caused by an incident wave at the base of the soil profile at -500m, (i.e. transfer function from point 1 to 4 in Fig. 3) are shown in Fig. 7 for different pile diameters. The height of the peak at 0.5 Hz (the first resonant frequency of the profile) decreases as the stiffness of the piles increases. However, this tendency is reversed at the second resonant frequency, at 1.1 Hz.

When mass is added to the pile foundation, the first resonant peak shifts to a lower frequency and increases in height, see Fig. 8. For simplicity, the mass is assumed rigid (eg. a very stiff shear wall building), and no rotation of the pile cap is considered.

Figures 7 and 8 suggest that a stiffer foundation (eg. larger piles) and a smaller building mass (eg. by excavation for basements) tend to reduce the motion of the pile foundation at the fundamental frequency of the soil profile, but may increase the response at higher frequencies.

ACKNOWLEDGEMENTS

Data on the earthquake of September 19, 1985 was generously provided by members of IdI, UNAM who were extremely helpful when the authors visited Mexico City briefly after the earthquake. Special thanks are extended to the Directorate-General for Science, Research and Development of the Commissionn of the European Communities and to Centro Nacional de Prevencion de Desastres (Mexico) who sponsor the workshop.

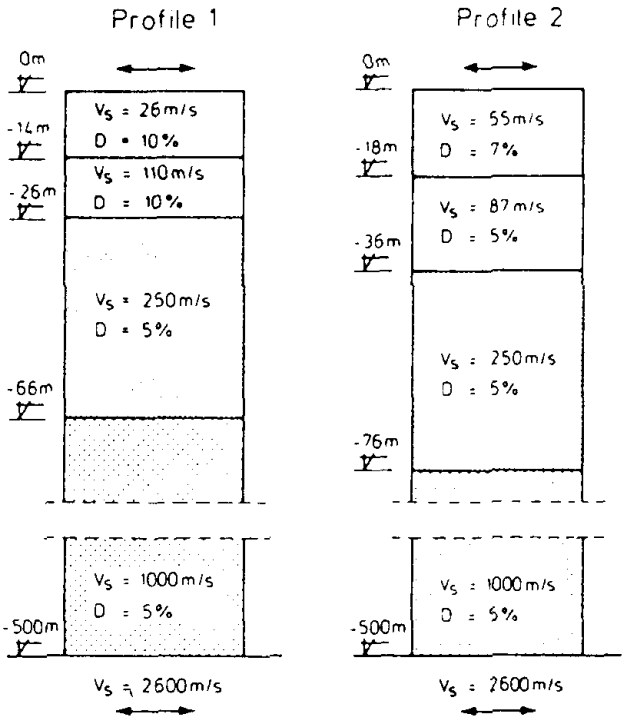

FIGURE 1. Profiles for amplification analysis, representative for the center of Mexico City

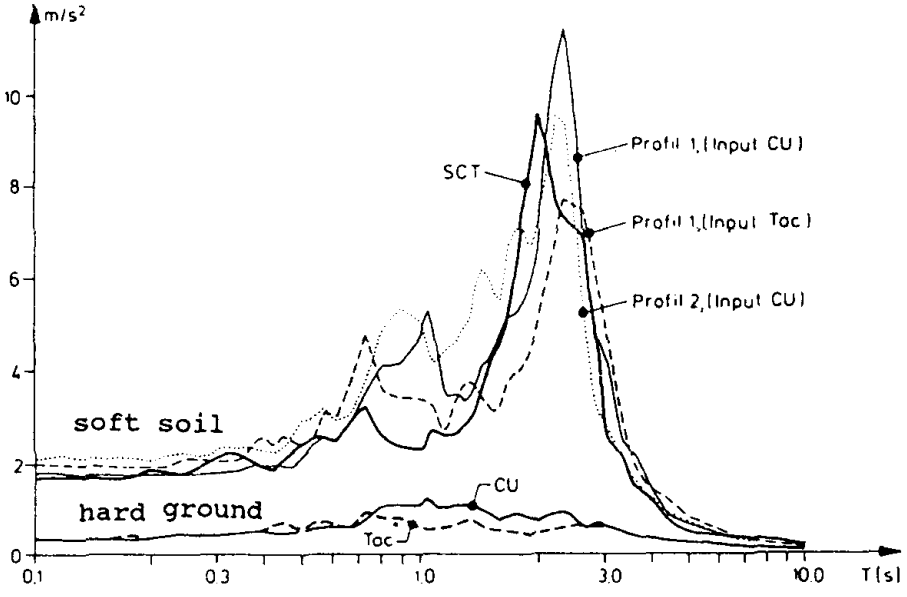

FIGURE 2. Response spectra of horizontal accelerations computed (Input Cu, Tac) and recorded, 5% damping

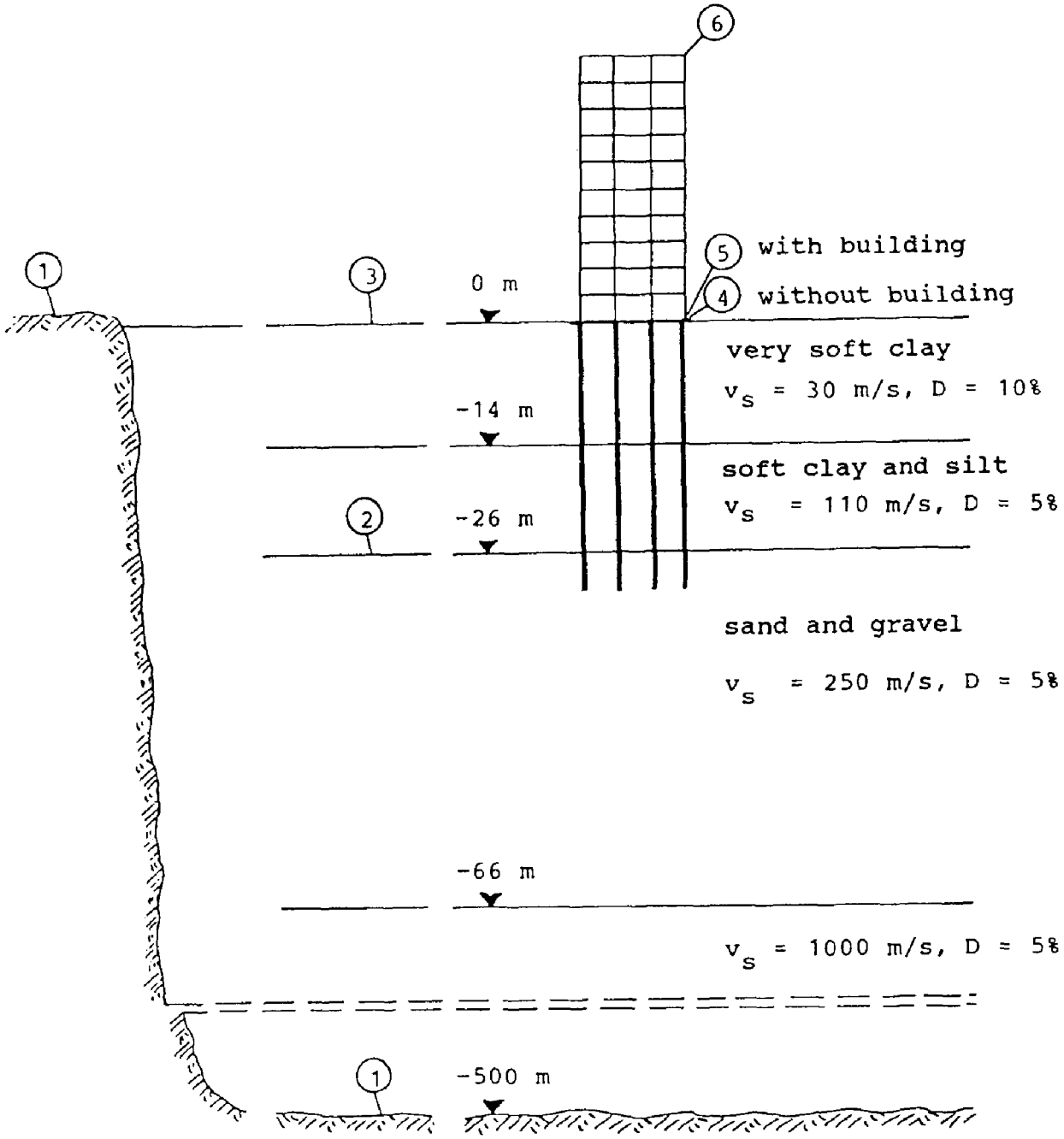

FIGURE 3. Office building on pile foundation with idealized geotechnical profile in the center of Mexico City

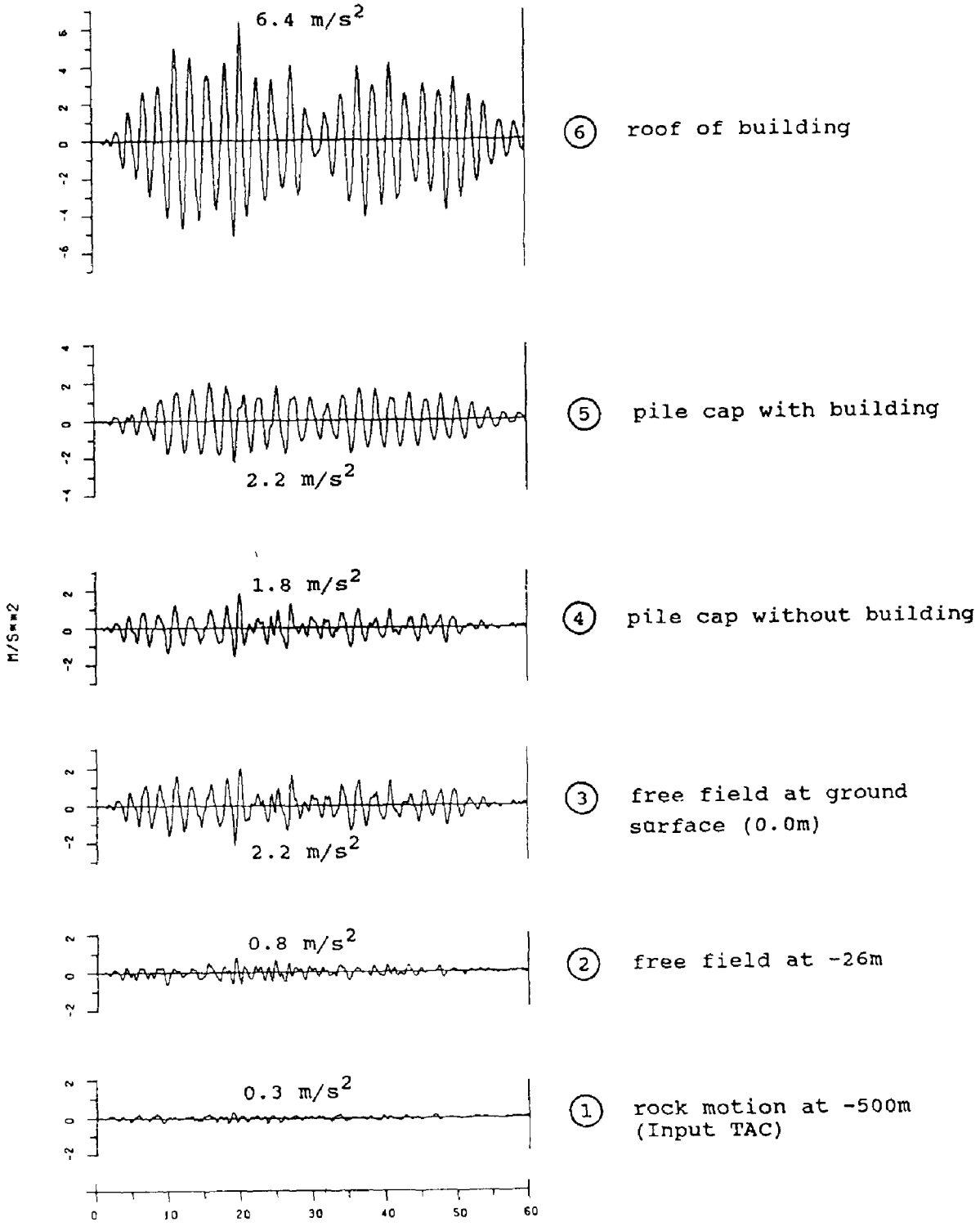

FIGURE 4. Horizontal accelerations for points in Fig. 4

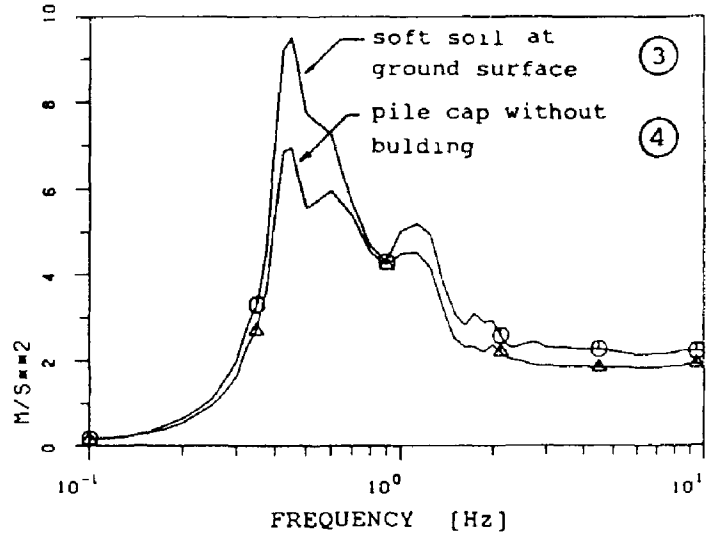

FIGURE 5. Response spectra for 5% damping

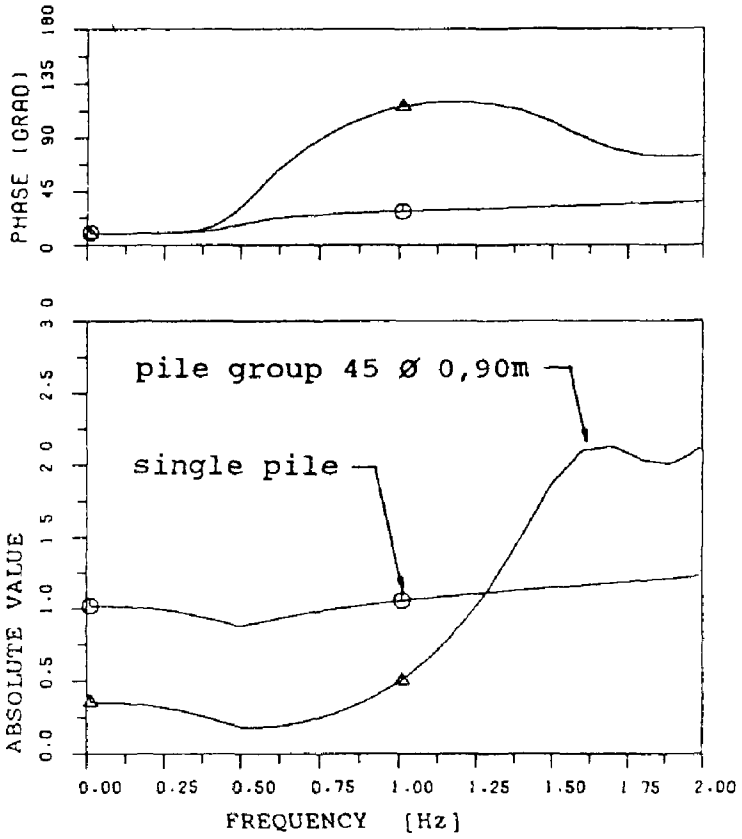

FIGURE 6. Dynamic horizontal stiffness of a single pile and a pile group in profile 1, related to static stiffness of a single pile

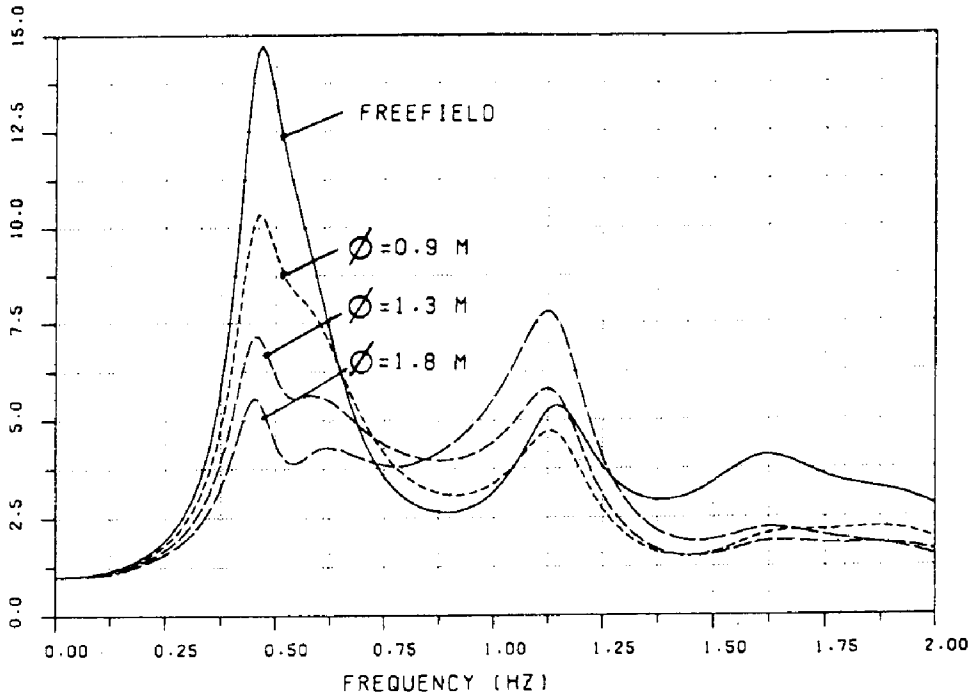

FIGURE 7. Transfer function of horizontal motion from base of profile 1 to pile foundation without building mass for different pile diameters

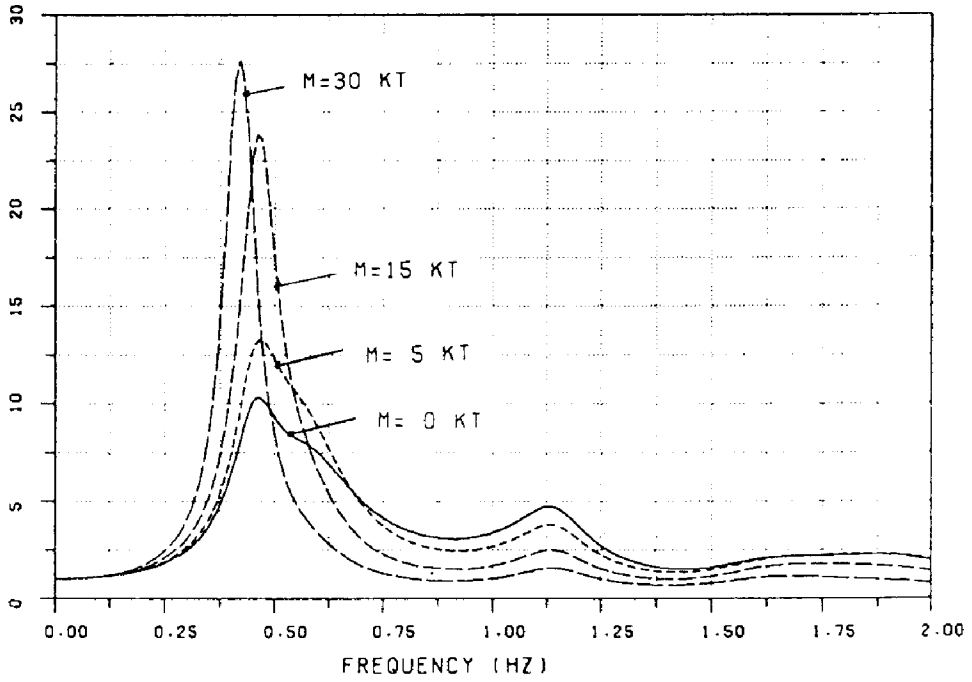

FIGURE 8. Transfer functions of horizontal motion from base of profile 1 to pile foundation with rigid mass for pile diameter of 0.9 m

REFERENCES

1. Hartmann, H.-G., "Pfahlgruppen in geschichtetem Boden unter horizontaler dynamischer Belastung", Dissertation, Technische Hochschule Darmstadt, 1986.

2. Rosenblueth, E., and Elordny, J., "Characteristic of earthquakes on Mexico City Clay", 1969.

3. Wass, G., "Linear two- dimensional analysis of soil dynamics problems in semi-infinite layered media". Dissertation, University of California, Berkeley, California, 1972.

4. Wass, G., "Dynamisch belastete Fundamente auf geschichtetem Baugraund", in VDI-Bericht 381, 1980.

5. Wass, G., Riggs, H.R., Werkle, H., "Displacement solutions for dynamic loads in transversely-isotropic stratified media", Earthquake Eng. and Str. Dynamics, Vol. 13, 1985.

TABLE 1. Static stiffness of single pile and group of 4 x 11 piles, spacing 5 m, motion in direction of short dimension

		1	2	3
Diameter of piles	m	0.90	1.30	1.80
Horizontal stiffness	MN/m			
single pile, profile 1		19.7	31.9	53.5
profile 2		44.9	69.9	103.2
group of 44, profile 1		310	524	912
group factor		0.35	0.37	0.38
profile 2		594	749	973
group factor		0.30	0.24	0.21
Rocking stiffness	MNm/rad			
group of 44, profile 1		533000	757000	963000

APPENDIX

Ring and Point Loads in a Layered Medium

The displacements of harmonic motion in a layered elastic or viscoelastic medium at frequency w may be represented in cylindrical coordinates, Fig. 3, using the following functions:

$e^{i\omega t}$ for the variation in time

$e^{i\nu\theta}$ for the variation in the hoop direction,

the Bessel functions $J\nu$ (kr) or $H\nu$ (kr) for the variation in the radial direction, and continuous piecewise linear functions in the z- direction. The functions in t, θ and r satisfy the respective ordinary differential equations, which are obtained by separation of variables from the equations of motion in cylindrical coordinates. The functions in z are approximations which require a subdivision of the natural soil layers into thin layers as dedicated in Fig. 3[3]. The number of layers be n.

Enforcing compatibility of displacements and equilibrium at the interfaces of the n soil layers and observing homogeneous boundary conditions (zero stresses at top and zero displacements at bottom) yield two eigenvalue problems [3] which can be solved easily. They depend on ω but are independent of ν . The homogeneous solution for motion in the r-z plane consist of 2 n generally complex wave numbers k_j and the eigenvectors X_j and Z_j containing the horizontal and vertical displacement components respectively. For motion in the r-θ plane one obtains n wave numbers k_j and the corresponding vectors Y_j.

The displacements u, v, w and the strains and stresses can now be expanded in terms of the eigensolutions. In order to compute the displacements caused by ring loads at distance R from the center line, see Fig. 3, one may consider a cylindrical surface at radius R. When computing displacements and stresses, one has to use the Bessel functions $J\nu$ for r < R due to the reflection at r = 0, and the Hankel function $H\nu^{(2)}$ for r >R, because amplitudes must decay with distance from R[5]. At the cylindrical surface r = R, internal stresses and external loads must be in equilibrium and displacements must be compatible. Enforcement yields the following results:

The displacements at a point (r, z = 1, θ) caused by a line load at the nodal ring (R, z=h), see Fig. 3, are.

$$u = \left[\sum_{j=1}^{2n} H_j' X_{1j} a_j + \sum_{j=1}^{n} \frac{\nu}{r} \bar{H}_j Y_{1j} c_j\right] \cdot \frac{-i}{4} \cos \nu\theta \cdot e^{i\omega t} \qquad (1)$$

$$v = \left[\sum_{j=1}^{2n} \frac{\nu}{r} H_j X_{1j} a_j + \sum_{j=1}^{n} \bar{H}_j' Y_{1j} c_j\right] \cdot \frac{i}{4} \sin \nu\theta \cdot e^{i\omega t} \qquad (2)$$

$$w = \left[\sum_{j=1}^{2n} k_j H_j Z_{1j} a_j\right] \frac{-i}{4} \cos \nu\theta \cdot e^{i\omega t} \qquad (3)$$

with

$$H_j = H_\nu^{(2)}(k_j r) \qquad H_j' = \frac{d}{dr} H_j$$
$$\bar{H}_j = H_\nu^{(2)}(\bar{k}_j r) \qquad \bar{H}_j' = \frac{d}{dr} \bar{H}_j \qquad (4)$$

For a ring load in r-direction $P_r = \cos \nu\theta / 2\pi R$

$$a_j = J_j' X_{hj} \qquad c_j = \bar{J}_j Y_{hj} \frac{\nu}{R} \qquad (5)$$

For a ring load in θ direction $P\theta = -\sin \nu\theta / 2\Pi R$

$$a_j = J_j X_{hj} \frac{\nu}{R} \qquad c_j = \bar{J}_j' Y_{hj} \qquad (6)$$

For a ring load in z-direction $Pz = \cos \nu\theta / 2\Pi R$

$$a_j = k_j J_j Z_{hj} \qquad c_j = o \qquad (7)$$

Eqs. 1 to 7 are valid for $r \geq R$ for $r < R$ Hankel and Bessel functions must be interchanged. The abbreviations with J_j correspond to those in Eq. 4. Normalization of X_j, Y_j and Z_j is understood as in [3] but with a subsequent division by $\bar{k}_j$ or k_j, respectively.

For $\nu = o$ the displacement-- is not coupled with u and w If in this case the sinus-function in Eq. 2 is replaced by 1, v will represent pure torsional motion.

When the radius R of the ring load goes to zero one obtains the displacements caused by a point load. For a horizontal point load $Px = 1$ in the x-direction (θ=o) is one and

$$a_j = k_j X_{hj} \qquad c_j = \bar{k}_j Y_{hj} \qquad (8)$$

For a vertical point load $Pz = 1$, ν is zero and .

$$a_j = k_j Z_{hj} \qquad c_j = o \qquad (9)$$

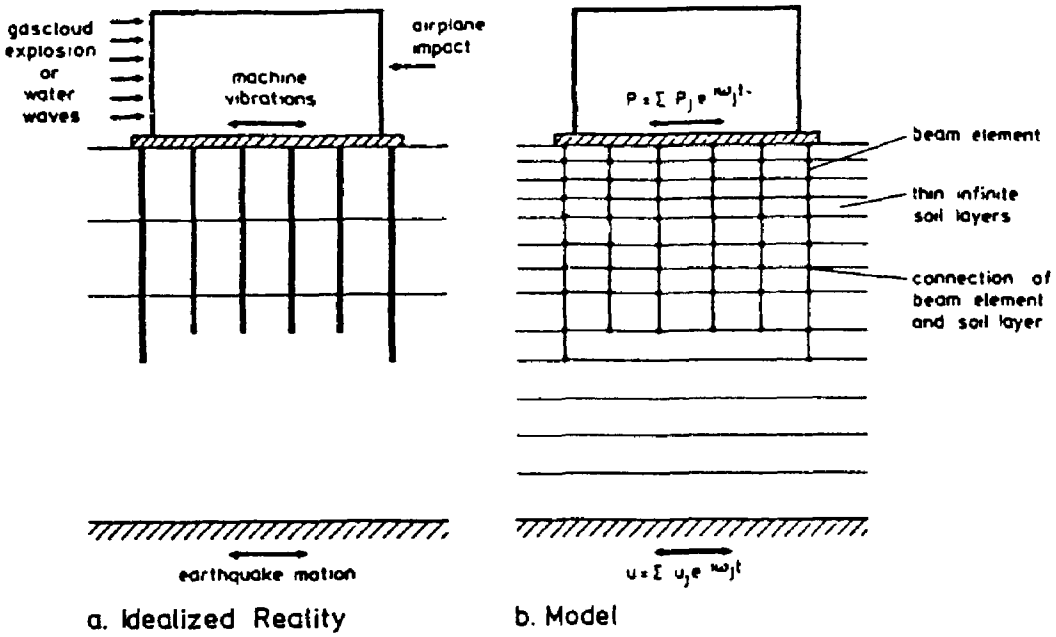

Fig. 1 Pile foundation subjected to horizontal dynamic loads

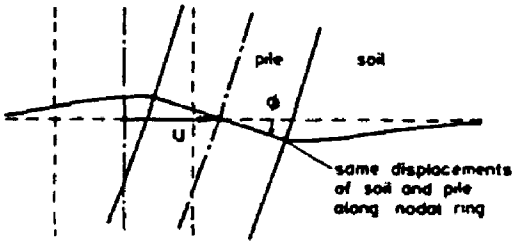

Fig. 2 Connection between pile and soil at interfaces of thin soil layers

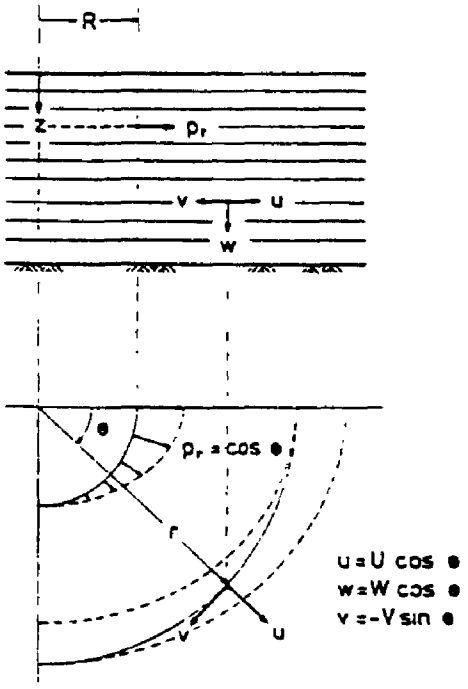

Fig. 3 Displacements in a horizontally layered medium caused by a horizontal ring load for $\nu = 1$